Experimental and computational thermomechanical study of a shape-memory alloy micro-actuator: aspects of antagonist-type behavior

R. Velázquez[a,*], M. Hafez[b], J. Szewczyk[a], E. Pissaloux[a]

[a]*Laboratoire de Robotique de Paris and CNRS FRE 2507, 18 Route du Panorama, BP 61, 92265 Fontenay aux Roses, France*
[b]*CEA/LIST, 18 Route du Panorama, BP 61, 92265 Fontenay aux Roses, France*

Abstract

A combined computational/experimental study of a shape-memory alloy (SMA) linear micro-actuator based on the working principle of antagonist configuration is presented. An electrically driven NiTi helical spring is used as the active element in such an actuator. The thermomechanical properties of the fabricated SMA spring were evaluated using a constitutive model and investigated experimentally through two types of tests: isothermal loading/unloading and fatigue due to plastic strain development. Both experimental and computational results are in good agreement and are used to characterize the actuator's SMA antagonist-type behavior.

Keywords: SMA; Helical spring; Antagonist actuator; Thermomechanical property; Fatigue

1. Introduction

Shape-memory alloys (SMAs) have several characteristics that make them attractive over other materials, especially for actuation applications: compact size, high power/weight ratio, high fatigue resistance to cyclic motion, and spark-free, clean, and noiseless operation [1]. Additionally, they have unique properties based on superelasticity and the shape-memory effect (SME).

The SME does not simply imply that the memory shape will be restored freely when the SMA is heated. Recovering a memory shape depends strongly on several thermomechanical parameters, such as temperature, pre-strain, number of loading cycles, strain rate, and stress level.

In order to design or to evaluate the performance of SMA elements, the understanding of the stress–strain–temperature dependence becomes important. In practice, this dependence determines the working characteristics of a SMA element: force, stroke, fatigue life, and set/reset points.

In this paper, the thermomechanical properties associated with the stress–strain–temperature relationship such as isothermal loading/unloading and fatigue failure due to strain amplitude are investigated for a NiTi helical spring. Computational analyses were performed to predict these behaviors and were validated by experimental results. Then, arranged in antagonist configuration, a pair of springs was used to build a linear motion micro-actuator. The SMA antagonist behavior, exploited widely in robotic applications, is characterized using the spring's thermomechanical properties.

The rest of this paper is organized as follows: the experimental environment employed in this study is described in Section 2. Section 3 presents both experimental and theoretical results on the thermomechanical properties of the SMA element. Based on these data, Section 4 formulates the SMA antagonist behavior. Section 5 concludes with the main concepts and results.

2. Experimental environment

2.1. Materials

A NiTi helical spring was fabricated with Flexinol™ wire with the following geometric characteristics: wire diameter 200 μm, mean spring diameter 1.3 mm, and 12 active coils.

* Corresponding author. Tel.: +33 146 549079; Fax: +33 146 547299; E-mail: velazquez@robot.jussieu.fr

Computational Fluid and Solid Mechanics 2005
K.J. Bathe (Editor)

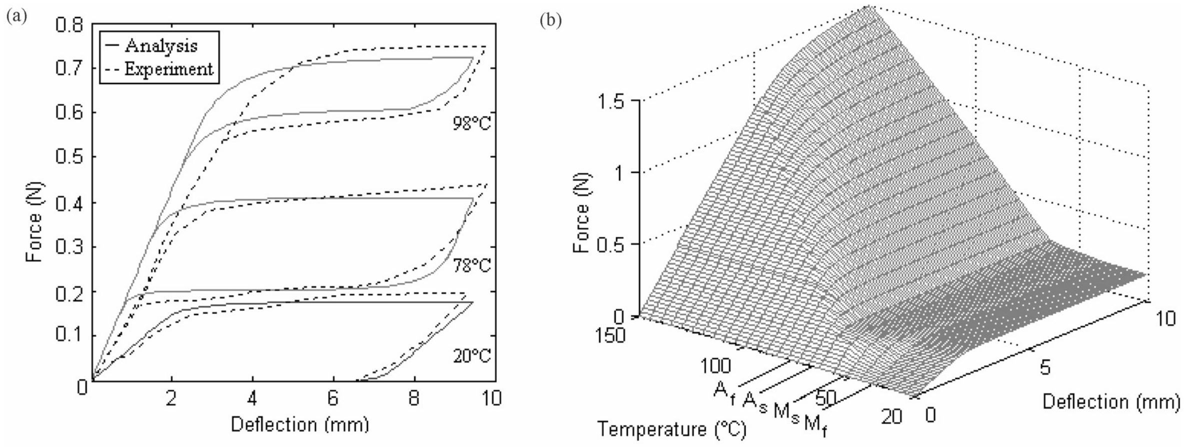

Fig. 1. (a) Force–deflection relations of the SMA spring at constant temperatures (20 °C, 78 °C, and 98 °C) and (b) the spring's SMA loading behavior in the force–deflection–temperature space.

Energy-dispersive X-ray (EDX) analysis confirmed its composition to be approximately $Ni_{52}Ti_{48}$. The helical spring shape was set through a heat treatment process in which the material was subjected to 500 °C for 5 min. Rapid cooling via water quenching concluded the process.

The transformation temperatures determined by a differential scanning calorimeter (DSC) are 78, 68, 52, and 42 °C for A_f, A_s, M_s, and M_f, respectively.

2.2. Testing apparatus

To investigate the thermomechanical properties of the SMA spring, two kinds of tests were performed: isothermal loading/unloading and fatigue due to plastic strain. Both tests were conducted using a tensile machine fitted with a linear variable differential transformer (LVDT), a load cell, and a thermocouple, to measure the deflection, the tensile force exerted, and the temperature of the spring, respectively.

3. Computational/experimental evaluation of shape-memory alloy thermomechanical properties

3.1. Isothermal loading/unloading

From Tobushi and Tanaka's elastoplastic model [2], torsional stress is a temperature-dependent parameter for an SMA helical spring. Based on this assumption, they proposed a one-dimensional force-deflection relation, which can be expressed as follows:

$$F = \begin{cases} \frac{Gd^4}{8ND^3}\delta & \text{for } \delta < \delta_e \\ \frac{\pi\tau_p d^3}{6D}\left[1 - \frac{1}{4}\left(\frac{\pi N \tau_p D^2}{dG\delta}\right)^3\right] & \text{for } \delta \geq \delta_e \end{cases}$$
$$\text{with}: \delta_e = \frac{\pi D^2 N \tau_p}{Gd} \text{ and } \tau_p = \begin{cases} c_M(T - M_s) \text{ for loading} \\ c_A(T - A_s) \text{ for unloading} \end{cases} \quad (1)$$

where F is the force developed by the SMA spring as a function of deflection δ, d is the wire diameter, D is the mean spring diameter, N is the number of active coils, G is the shear modulus of elasticity, τ_p is the maximum torsional stress, δ_e is the boundary of elastic and plastic regions, and c_M and c_A are the material's constants, which describe the transformation conditions.

For NiTi, the experimental data of Birman [3] indicate austenitic $G = 28.2$ GPa and martensitic $G = 10.5$ GPa, while those of Tobushi and Tanaka [2] estimate $c_M = 6.3$ MPa/K and $c_A = 4.9$ MPa/K.

Fig. 1a compares the calculated and experimental force–deflection curves for a maximum deflection of 10 mm. Both simulation and experimentation were performed for each material phase independently, i.e. pure austenitic and pure martensitic loading/unloading under isothermal conditions (20, 78, and 98 °C).

As found from Fig. 1a, simulation characterizes well the overall deformation behavior. It should be noted that the force developed by the spring increases with temperature. However, the unloading curves indicate the mechanical hysteresis of the SMA when the memory shape is being recovered. Note that for temperatures at or above the austenite state, the memory shape is recovered perfectly, but for martensite states, it does not.

Fig. 1b shows the phenomenological representation of

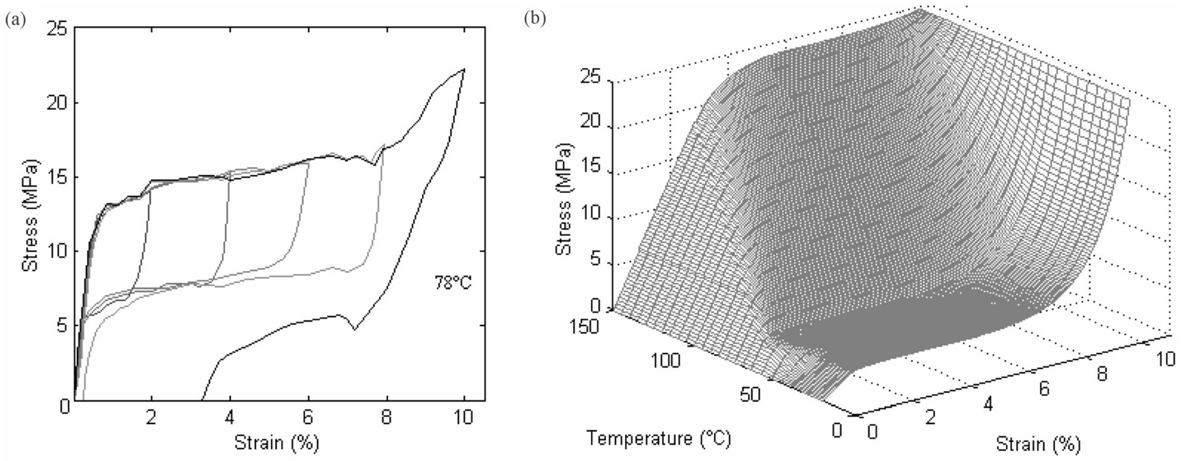

Fig. 2. (a) Stress-strain experimental results for austenitic plastic strain developed and (b) computational stress–strain–temperature behavior for martensitic/austenitic plastic deformation in loading.

the spring's SMA behavior in the force–deflection–temperature space.

3.2. Fatigue

In practice, SMAs are required to perform in cyclic motion. This implies that SMAs are subjected to both mechanical and thermal cycling with repeated loading/unloading and heating/cooling.

When subjected to thermomechanical cycling, shape-memory properties are affected, in particular the SME. From a material point of view, fatigue introduces defects such as dislocations that tend to soften and create fissures in the alloy, eventually ending in the rupture of the material [4].

To avoid or delay this degradation, it is convenient to study the fatigue properties of the material. This paper evaluates the relationship between strain amplitude and fatigue.

When an SMA is loaded repeatedly in the austenite phase, with a gradual increase of the total applied strain, the effect of accumulated plastic strain affects the phase-transformation characteristics at some point. It becomes essential to determine this point in order to limit the strain amplitude applied to the SMA.

Fig. 2a shows the stress–strain relationship of the SMA spring. Tests were performed at 78 °C (A_f) as complete loading/unloading cycles. Each cycle is repeated several times, incrementing the total strain by 2% (a 10-mm deflection step) for each loading. The effects of plastic strain on the transformation characteristics of the spring are quantified by measurement of the recoverable strain under zero applied stress for each mechanical cycle. Experimental results show that the memory shape is recovered for plastic strains at 2%, 4%, and 6%. However, at 8%, the spring begins to lose its SME slightly; 10% strains produce a complete loss of actuation.

Fig. 2b proposes a computational behavior of the spring's plasticity in the stress–strain–temperature space. Note that although stress–strain curves are different at various temperatures, plastic strain limit is almost the same [5].

The number of cycles to failure associated to plastic strain are typically quoted as follows: 1 cycle for strains at 8%, 10^2 cycles for strains at 4%, 10^4 cycles for strains at 2%, and more than 10^5 cycles for strains at 1% [6]. In order to obtain the maximum fatigue life, the spring should be actuated up to a 5-mm deflection.

4. Shape-memory alloy antagonist behavior

Although an SMA spring could be designed such that it exerts a force in three dimensions, the great majority of SMA springs apply a one-directional tensile force and cannot directly apply a compressive force. It is then necessary to provide a biasing force to make them return to the initial position. In many robotic applications, a second SMA element arranged in antagonist mode is a widely exploited technique to obtain reversible motion of an SMA.

From a thermal point of view, the antagonist principle is based on heating one SMA element at a time, so that its austenitic state produces a force and displacement over the second martensitic SMA.

To investigate the SMA antagonist behavior, a linear micro-actuator (cf. Fig. 3) was built with a pair of SMA springs of geometric and thermomechanical

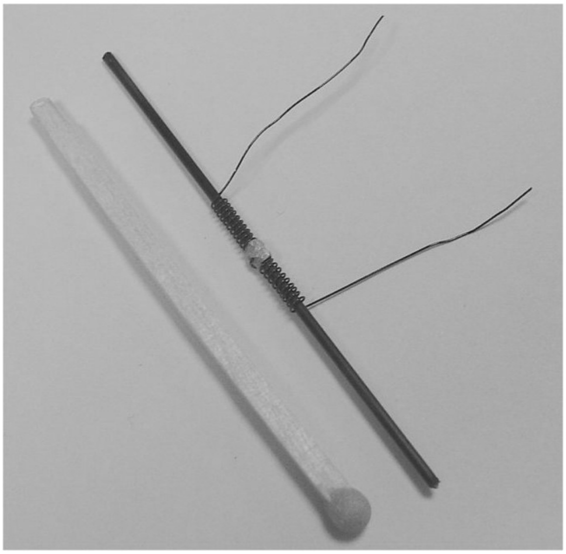

Fig. 3. SMA helical spring-based micro-actuator.

characteristics described so far. Consider both springs identically pre-strained (distance O–δ_0 and O'–δ_o in Fig. 4a) in martensitic equilibrium point δ_0 (Fig. 4a(1)). When the lower spring is heated, the new equilibrium point B is defined by the intersection of its austenite curve and the upper spring's martensite curve (Fig. 4a(2)). When cooling, the lower spring tends to recover its martensite characteristic at the same time that the upper spring mechanically unloads. As seen, the equilibrium point does not follow the B–δ_0 trajectory but the B–D trajectory (Fig. 4a(3)). The same phenomenon is observed when the upper spring is heated; it follows δ_0/D–A–C instead of δ_0/D–A–δ_0 (Figs. 4a(4) and 4a(5)).

A more complete representation of the thermomechanical path followed by the equilibrium point is shown in Fig. 4b. Note that the initial position δ_0 is not recovered due to the mechanical unloading characteristic of martensite.

A second case is when one of the springs is kept passive in the austenite state while the other is activated from martensite to austenite (Fig. 5a). Note that the superelasticity property appears in both active and passive springs in order to reach point δ_0. When cooled, the passive spring mechanically unloads by following its austenite characteristic (Fig. 5b). Note that the initial position A is recovered in this case, even though a non-reversible path is observed between A–δ_0.

5. Conclusion

This paper has presented a computational/experimental study on the thermomechanical properties of a NiTi helical spring and its application to the characterization of SMA antagonist actuators. In particular, the stress–strain–temperature relationship was investigated through isothermal loading/unloading and fatigue tensile tests. The main results are summarized as follows:

1. The proposed analytical force–deflection relation represents sufficiently closely the system's physical performance.
2. The analysis of the influence of plastic strain permits us to establish the spring's operating stroke in order to obtain a maximum number of cycles.
3. When arranged in antagonist configuration, its mechanical characteristic produces a system with two equilibrium points (C and D) in which the starting point δ_0 is never recovered.

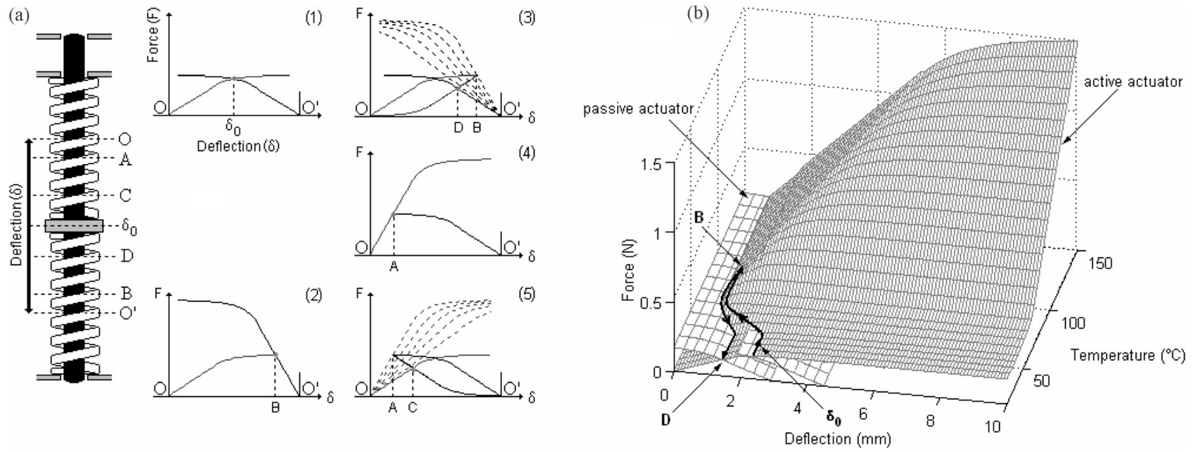

Fig. 4. SMA antagonist principle: (a) the actuator's conceptual representation and force-deflection relations for a complete operating cycle; (b) thermomechanical path performed by a spring in the force–deflection–temperature space.

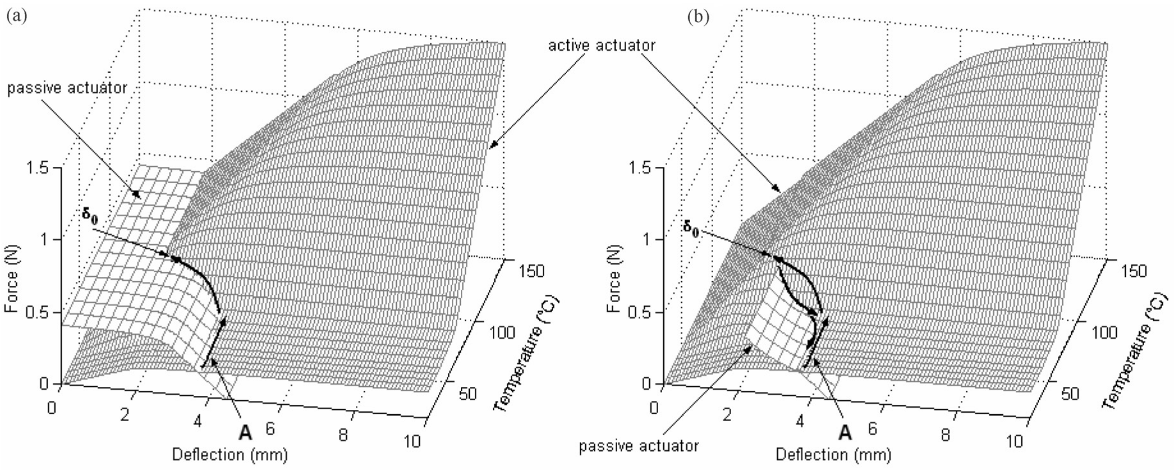

Fig. 5. Antagonist operation with a passive austenitic spring: active spring's behavior at (a) set and (b) reset points.

This micro-actuator is currently being used to design and develop high-resolution, light-weight, and compact interfaces for tactile information display [7].

References

[1] Ikuta K. Micro/miniature shape memory alloy actuator. In: Proceedings of IEEE International Conference on Robotics and Automation, Cincinnati, USA, IEEE Robotics & Automation Society, editor, Piscataway, NJ, IEEE Press, 1990, pp. 2156–2161.

[2] Tobushi H, Tanaka K. Deformation of a SMA helical spring. JSME Int J 1991;34:83–89.

[3] Birman V. Review of mechanics of shape memory alloy structures. Appl Mech Rev 1997;50:629–645.

[4] Miller D, Lagoudas D. Thermomechanical characterization of NiTiCu and NiTi SMA actuators: influence of plastic strains. Smart Mater Struct 2000;9:640–652.

[5] Tobushi H, Nakahara T, Shimeno Y, Hashimoto T. Low-cycle fatigue of TiNi shape memory alloy and formulation of fatigue life. J Engng Mater Technol 2000;122:186–191.

[6] Dynalloy Inc. Flexinol data sheet. Updated information available at www.dynalloy.com

[7] Velázquez R, Pissaloux E, Szewczyk J, Hafez M. Design and characterization of a shape memory alloy based micro-actuator for tactile stimulation. In: Proceedings of IEEE International Symposium on Industrial Electronics, Ajaccio, France, IEEE Industrial Electronics Society, editor, IEEE Press, Piscataway, NJ, 2004, pp. 3–8.